Published online 10 July 2017

Nucleic Acids Research, 2017, Vol. 45, No. 17 ***9931–9946***
doi: 10.1093/nar/gkx589

Dual function of Swc5 in SWR remodeling ATPase activation and histone H2A eviction

Lu Sun and Ed Luk*

Department of Biochemistry and Cell Biology, Stony Brook University, NY 11794-5215, USA

Received March 07, 2017; Revised June 19, 2017; Editorial Decision June 24, 2017; Accepted June 29, 2017

ABSTRACT

The chromatin remodeler SWR deposits histone H2A.Z at promoters and other regulatory sites via an ATP-driven histone exchange reaction that replaces nucleosomal H2A with H2A.Z. Simultaneous binding of SWR to both H2A nucleosome and free H2A.Z induces SWR ATPase activity and engages the histone exchange mechanism. Swc5 is a conserved subunit of the 14-polypeptide SWR complex that is required for the histone exchange reaction, but its molecular role is unknown. We found that Swc5, although not required for substrate binding, is required for SWR ATPase stimulation, suggesting that Swc5 is required to couple substrate recognition to ATPase activation. A biochemical complementation assay was developed to show that a unique, conserved domain at the C-terminus of Swc5, called Bucentaur (BCNT), is essential for the histone exchange activity of SWR, whereas an acidic region at the N-terminus is required for optimal SWR function. *In vitro* studies showed the acidic N-terminus of Swc5 preferentially binds to the H2A–H2B dimer and exhibits histone chaperone activity. We propose that an auxiliary function of Swc5 in SWR is to assist H2A ejection as H2A.Z is inserted into the nucleosome.

INTRODUCTION

The regulation of chromatin structure and dynamics plays a fundamental role in the control of genome processes. The unit building block of chromatin is the nucleosome (1). Within a typical nucleosome is a modular, octameric protein core made up of a tetramer of histones H3 and H4 [referred to as $(H3\text{-}H4)_2$] sandwiched by two dimers of histones H2A and H2B [referred to as (H2A–H2B)] (2). The resulting puck-like core is wrapped around 1.7 times by ∼150 base pairs (bp) of DNA forming a left-handed solenoid (3). The formation of nucleosomes and the arrangement of nucleosomes into closely spaced arrays render the underlying DNA sequences largely inaccessible to most DNA binding factors (4). By controlling the position and occupancy of nucleosome along the chromosomes, transcription factors are excluded from inactive promoters and cryptic promoter-like sequences but are drawn to exposed DNA elements defined by the flanking nucleosomes to allow accurate, focused assembly (5–7). ATP-dependent chromatin remodelers utilize the energy from ATP hydrolysis to drive histone movement along or in-and-out of DNA and thus play a key role in the establishment and maintenance of the nucleosome organization (8,9). Guided by DNA elements and sequence-specific factors, remodelers clear nucleosomes around promoters to create nucleosome free regions (NFRs) that serve as the platform for the transcription machinery assembly (7,8,10–12). The nucleosome immediately downstream of the NFR, called +1, is precisely positioned by the opposing sliding action of remodelers (8,11,13,14). In yeast, the upstream edge of the +1 nucleosome covers the transcription start site (15). The accurate positioning of the +1 nucleosome is functionally important as remodeler mutants that shift the position of the +1 nucleosome lead to aberrant start site selection (13).

Another unique feature of +1 nucleosomes is that they are frequently assembled with the histone variant, H2A.Z, instead of H2A (15,16). H2A.Z is essential for life in metazoans (17,18). Yeast cells deleted for *HTZ1* (the gene that encodes H2A.Z) are viable but exhibit growth defects and loss of fitness under stress (19). Although H2A.Z is not required for the steady-state transcript output of most genes, it is required for rapid transcriptional induction, including the heat-shock and the cyclin genes, and is preferentially evicted (over H2A) from promoters during gene activation (20–23). One hypothesized function of H2A.Z is that it forms a nucleosome that is poised or recognized for disassembly, thereby allowing a rapid transcriptional response (23). Consistent with this idea, +1 H2A.Z nucleosomes are rapidly turned over with an occupancy half-life of <15 min at most promoters, including those that are infrequently transcribed, suggesting that the +1 nucleosomes are subjected to constitutive remodeling activities that promote nucleosome disassembly (24,25). Although previous studies suggested that the INO80 chromatin remodeler was responsible for H2A.Z eviction, subsequent studies have demonstrated that the major contribution of H2A.Z evic-

*To whom correspondence should be addressed. Tel: +1 631 632 1903; Email: ed.luk@stonybrook.edu

tion comes from the assembly and/or the activity of the transcription machinery (25–27).

H2A.Z is deposited into +1 nucleosomes by the SWR1 complex (referred to as SWR hereafter), a member of the ATP-dependent chromatin remodeler family (19,21,28). Unlike other remodelers, SWR does not cause a net change in histone octamer position or net loss of histones *in vitro*; instead it catalyzes a histone exchange reaction that replaces nucleosomal H2A–H2B with free H2A.Z–H2B dimers delivered to the remodeler by one of several histone chaperones, such as Chz1, Nap1 and FACT (21,29,30). The directionality of the reaction is ensured by the regulation of the SWR ATPase that becomes hyper-stimulated when simultaneously bound to both histone substrates, i.e. the H2A-containing nucleosome and the H2A.Z–H2B dimer(s) (31). A fundamental question is how SWR recognizes the correct *in vivo* substrates, activates its ATPase and engages the histone exchange mechanism.

The eviction of the nucleosomal H2A–H2B is coupled to the insertion of H2A.Z–H2B, as demonstrated by the *in vitro* experiments showing that H2A.Z–H2B is required for full stimulation of the SWR complex ATPase, as well as the eviction of the nucleosomal H2A–H2B (31). After the first round of histone exchange, the SWR complex must then engage with the second H2A–H2B dimer on the opposite face of the nucleosome and replace it with H2A.Z–H2B. As such, SWR converts a homotypic H2A/H2A (AA) nucleosome to the heterotypic H2A.Z/H2A (AZ) form before generating the homotypic H2A.Z/H2A.Z (ZZ) nucleosomal product (31) (Supplementary Figure S1A).

The SWR complex, which weighs over one megadalton, is comprised of the Swr1 core ATPase plus associating factors encoded by 13 other genes (19,21,28,32). How these other proteins interact with the Swr1 ATPase motor, a DEAD-box super family (SF) 2 translocase, to coordinate histone exchange is unclear. The Swr1 polypeptide also serves as a scaffold for the assembly of the other subunits, which are organized into structurally distinct modules (33,34) (Supplementary Figure S1B, Swr1 in *blue*). The 'N-module' (in *pink*) is associated with the N-terminus of Swr1 and consists of Bdf1, Yaf9, Swc4, Swc7, Arp4 and Act1 (34). Several of these subunits are histone code readers. For example, Bdf1, which contains tandem bromodomains, binds preferentially to the tetra-acetylated histone H4 tail (35). The YEATS-domain containing Yaf9 binds to acetylated and crotonylated histone H3 (36,37). The actin-related protein Arp4 binds to phosphorylated H2A at serine 129, a mark linked to DNA damage response (38).

The C-terminal half of Swr1 bears a 'split' ATPase domain, which differs from the SF2 ATPase domains found in other remodelers in that a much longer insert domain links the two RecA-like protein folds of the predicted ATPase motor structure (39) (Supplementary Figure S1B, *dark blue*). Two other subunit modules, namely the 'C-module' and the 'Rvb1/2-module', require the insert domain to dock onto the Swr1 ATPase (33,34) (Supplementary Figure S1B, C-module in *yellow*; Rvb1/2 in *purple*). The Rvb1/2-module is a AAA+ heterohexameric ring formed by the RuvB-related ATPases, Rvb1 and Rvb2 (40,41). Electron microscopy analysis indicated that the Rvb1/2 ring interacts with the N-module, C-module, and the Swr1 scaffold, suggesting that it could serve as an organization platform (not depicted in Supplementary Figure S1B for simplicity) (33).

The C-module contains the subunits Swc2, Swc6, Arp6, and Swc3 (34) (Supplementary Figure S1B). Swc2 requires Swc6 and Arp6 for stable association with Swr1, and all three are essential for H2A.Z deposition *in vitro*, whereas Swc3 is not (34). Swc2, the second largest subunit of SWR after Swr1, has an integral role in the H2A.Z deposition mechanism. A conserved acidic region in Swc2 and in its human ortholog YL1, called the Swc2-Z or YL1-Z domain, preferentially binds to the H2A.Z–H2B substrate and is required for the H2A.Z deposition activity (34,42). Swc2 is also important for the targeting of SWR to the NFR to allow promoter-specific deposition of H2A.Z at the +1 positions (32). This targeting occurs via a conserved basic region that is adjacent to the Swc2-Z domain and is responsible for sensing the long DNA linker that protrudes from the nucleosome (32).

Swc5 is an 'orphan' subunit of SWR in that it is not an integral component of the C-, N- or Rvb1/2 modules (Supplementary Figure S1B, oval in cyan). Swc5 is required for the SWR-mediated H2A.Z deposition *in vivo* and *in vitro*, but its molecular role in the histone exchange process is unknown (25,34). SWR purified from *swc5Δ* cells contains all the subunits except Swc5, indicating that Swc5 is not necessary for the other subunits to bind to the Swr1 scaffold (34). However, stable interaction of Swc5 with the Swr1 scaffold requires the docking region of the N-module and the C-terminus of Swr1 (33,34,43,44).

In this study, we uncovered how Swc5 is involved in the SWR-mediated histone exchange process. First, Swc5 is required for the activation of the ATPase of SWR when the remodeler is bound to the H2A nucleosome and H2A.Z–H2B dimer, suggesting that it couples substrate recognition to DNA translocation activity. Second, Swc5 preferentially binds to H2A–H2B dimer, presumably to facilitate the ejection step of the histone exchange process. Domain analysis showed the BCNT domain is indispensable for the histone exchange activity, whereas the acidic N-terminus is involved in H2A–H2B binding but is only required for optimal exchange activity.

MATERIALS AND METHODS

Yeast strains and culture conditions

The genotypes of the yeast strains used in this study are listed in Supplementary Table S1. The yeast strains *SWR1–3xFLAG htz1Δ* (yEL190) and *SWR1–3xFLAG swc5Δ htz1Δ* (yEL291) used for native SWR purification are gifts from Carl Wu. The strain *swc5Δ* (Clone ID: 3371) (yEL274) was purchased from *GE Dharmacon*.

The yeast cultures used for native SWR purification were cultivated in 6 × 2 L yeast extract peptone dextrose (YPD) medium to an optical density (OD_{600}) of 2–4 before being harvested by centrifugation. The cell pellets were washed once with water and once with buffer A [300 mM HEPES–KOH (pH 7.6), 40% glycerol, 2 mM EDTA, 100 mM KCl] at 4°C. The packed-cell volume (PCV) was noted after centrifugation. After stirring the cells into a cell paste in the residual buffer A, the cells were frozen into 'nuggets' by

dripping into liquid nitrogen. The frozen yeast nuggets were stored at –80°C until ready for protein extraction.

Spotting assays were performed using wild-type (BY4741) or the isogenic *swc5Δ* haploid yeast (yEL274) transformed with a *CEN ARS URA3* vector (pRS416) bearing the wild-type *SWC5* or the mutant variants (45). The *SWC5* gene and the mutants were under the control of the endogenous promoter and terminator. Ten microliters of cell suspension at 1 OD_{600} and 10-fold serial diluents were seeded onto a synthetic complete medium lacking uracil in the presence or absence of 3% (v/v) formamide. The plates were incubated at 30°C for 2 days before imaged by the LAS4010 CCD camera (*GE Healthcare*).

Plasmid construction

A summary description of the plasmids used in this study can be found in Supplementary Table S2. The bacterial expression vector of yeast *SWC5* (pEL340) was a gift from Carl Wu. The *SWC5* gene in this vector is fused in-frame with the N-terminal 6x histidine/thrombin tag in the pET28c(+) vector. For the *swc5 (79–303)* and the *swc5 (147–303)* expression vectors, the *SWC5* gene fragments were synthesized by *Genscript*. The fragments were engineered to be flanked by NdeI and XhoI sites to allow subcloning into the pET28c(+) so that the *SWC5* sequences were in-frame with the N-terminal 6x histidine/thrombin tag. To generate the bacterial expression vectors for the C-terminal truncation mutants [*swc5 (1–254*)* and *swc5 (1–232*)*] and the alanine mutants [*swc5(FAGE→4A)*, *swc5(TTLEKS→6A)* and *swc5(LDW→3A)*], site-directed mutagenesis was used to introduce stop codons and alanine codons at the desired positions.

To generate the *SWC5* vector (pEL460) for the genetic complementation experiment, the *SWC5* gene, including 450 bp upstream of the start codon and 386 bp downstream of the stop codon, was amplified from yeast genomic DNA by PCR. The resulting PCR fragment was flanked by sequences that are homologous to the flanking regions immediately adjacent to the XhoI and EcoRI sites in the vector pRS416. After digesting with XhoI and EcoRI, the pRS416 vector was incubated with the *SWC5* gene fragment in the Gibson Assembly reagents to allow homologous recombination (*New England Biolabs*). The C-terminal truncation mutants and the alanine mutants for the yeast expression vectors were constructed by site-directed mutagenesis as described above. To construct the N-terminal truncation mutants, *swc5 (79–303)* and *swc5 (147–303)*, the sequence around the *SWC5* start codon (taaATG) in pEL460 was mutated to an EcoRI site (gaattc) generating the plasmid pEL483. The truncated *SWC5* genes were amplified by PCR, in which the primers covering the 5′-UTR were fused directly to an ATG followed by the first codon of the truncated sequence. The PCR fragments for *swc5 (79–303)* and *swc5 (147–303)* were then subcloned into pEL483 by Gibson Assembly via the EcoRI/BclI sites and EcoRI/SalI sites, respectively. The integrity of all *SWC5* sequences and the presence of mutations were confirmed by Sanger sequencing (*Genewiz*).

Purification of native SWR complexes from yeast

The wild-type SWR and the mutant SWR[swc5Δ] complexes were purified by affinity chromatography using the 3xFLAG epitope at the C-terminus of Swr1 followed by glycerol gradient sedimentation as previously described with some modifications (31). Twelve-liter culture equivalents of frozen yeast nuggets prepared as described above were pulverized under liquid nitrogen in a Freezer Mill (*SPEX*) at maximum speed 15 times for 1 min with 1 min pause between each cycle. The lysate was thawed by the addition of two PCV of buffer B [150 mM HEPES–KOH (pH 7.6), 20% glycerol, 1 mM EDTA, 50 mM KCl, plus 1× protease inhibitors (PI, which consists of 1.7 mg/ml PMSF, 3.3 mg/ml benzamidine hydrochloride, 0.1 mg/ml pepstatin A, 0.1 mg/ml leupeptin, 0.1 mg/ml chymostatin)]. After the addition of 0.2 M KCl, the lysate was incubated at 4°C with gentle mixing for 30 min to facilitate extraction. The extract was cleared by centrifugation at 83 000 x g in a SW28 rotor and was stored at –80°C until ready for affinity chromatography.

For FLAG affinity chromatography, thawed extract from 12-L equivalent of cells was thawed and incubated with 5-ml bed volume of anti-FLAG M2 agarose (*Sigma-Aldrich*) for 4 h at 4°C. The resin was washed twice with buffer C [25 mM HEPES–KOH pH 7.6, 1 mM EDTA, 10% glycerol, 0.01% NP-40, 0.2 M KCl, 2 mM $MgCl_2$, 1 mM $CaCl_2$ and 1× PI]. DNA was removed by digestion on the resin with 20 U/ml of DNase I (*Worthington*) in the presence of 10 mM $MnCl_2$ for 30 min at 4°C. The bead-bound SWR was washed with buffer D [25 mM HEPES–KOH pH 7.6, 1 mM EDTA, 10% glycerol, 0.01% NP-40, 0.5 M KCl and 1× PI] and with buffer E [same as buffer D, except that the 0.5 M KCl is replaced by 0.3 M NaCl] before elution with 0.5 μg/μl 3xFLAG peptide (*Sigma-Aldrich*) in buffer E at 4°C for 2 hours. The eluate was concentrated on a 10 kD MWCO centricon column (*EMD Millipore*) and then applied to a 15–40% glycerol gradient in buffer F [25 mM HEPES–KOH pH 7.6, 1 mM EDTA, 0.01% NP-40, 0.3 M NaCl] for velocity sedimentation. Centrifugation was performed at 192 000 × g at 4°C for 10 hours in a SW-55.1 rotor (*Beckman Coulter*). Peak fractions were detected by SDS-PAGE and SYPRO Ruby or silver staining and combined before being aliquoted for storage at –80°C. Protein concentration was determined by densitometric measurement of the Swr1 polypeptide band against a serially diluted BSA standard in SDS-PAGE.

Purification of recombinant Swc5 and swc5 mutant proteins for *in vitro* assays

To purify the recombinant Swc5 and mutant variants, transformants of the BL21(DE3) CodonPlus cells (*Agilent Technologies*) or the BL21(DE3) pLysS cells (*Promega*) bearing the corresponding bacterial expression vectors were cultivated in 1 L of the superbroth medium at 37°C until the OD_{600} reached 0.5. Induction was initiated by the addition of 0.2 mM isopropyl β-D-1-thiogalactopyranoside (IPTG) and was allowed to proceed for 4.5 h at 37°C. The cells were harvested by centrifugation, washed and resuspended in buffer G [20 mM Tris–HCl pH 7.9, 5 mM imidazole, 0.5 M NaCl, 7 M urea, 0.2 mM PMSF, 0.5% Triton X-20]. All

steps from this point onward were performed at 4°C. Cells were lysed by sonication (12 × 15-s pulses at 60% power with 30-sec pauses in between) in a Qsonica Q500 ultrasonic processor equipped with a 12.7 mm probe. The lysate was cleared by centrifugation at 19 710 × g in the JA-25.50 rotor for 30 min at 4°C before application into a 10-ml TALON Superflow cobalt column (*Clontech*). The resin was washed with buffer G and the Swc5 proteins were eluted in buffer I [20 mM Tris–HCl pH 7.9, 60 mM Imidazole, 0.5 M NaCl]. The fractions containing the Swc5 proteins were further purified on a 5-ml high performance Q Sepharose column with a 0.1–0.5 M NaCl linear gradient in buffer J [20 mM Tris–HCl pH 7.5]. After the peak fractions were concentrated by centrifugation in a 10 kD MWCO centricon column, the proteins were purified on a Superdex 200 Increase 10/300 GL column in eluent buffer K [20 mM Tris–HCl pH 7.5, 10% glycerol, 0.3 M NaCl].

For thrombin digestion, the His-tagged Swc5 proteins were incubated with 0.02 U/μL of thrombin (*GE Healtlhcare*) overnight at 4°C. The cleaved proteins were purified on the Superdex 200 column as described above.

Reconstitution of the remodeling substrates of SWR

Nucleosomes were reconstituted with recombinant yeast histone octamers and 204-bp Cy3-labeled DNA molecules bearing the Widom-601 sequence as described but with some modifications (46,47). The full sequence of the DNA fragment can be found in Supporting material S1. Briefly, the histone octamers were reconstituted from unfolded yeast H2A, H2B, H3, and H4 in buffer L [7 M urea, 10 mM Tris–HCl (pH 8.0), 1mM EDTA, 0.2 M NaCl, 5 mM 2-mercaptoethanol and 0.2 mM PMSF] by dialysis against buffer M [2 M NaCl, 10 mM Tris–HCl (pH 7.5), 1 mM EDTA, and 5 mM 2-mercaptoethanol] (47). The octamers were then purified by gel filtration on the Superdex 200 column using buffer M (but without 2-mercaptoethanol) as eluent. The Cy3-labeled 204 bp DNA was synthesized by PCR using primers 5′-[Cy3] TCT TCA CAC CGA GTT CAT CCC TT-3′ (forward) and 5′-TAC ATG CAC AGG ATG TAT ATA TCT GAC-3′ (reverse), and the 601 DNA fragment as template (Supporting material S1) (48). The unlabeled DNA used in the ATPase reactions was synthesized similarly by using the same forward primer but without the Cy3. All DNA fragments were cleaned up by standard phenol-chloroform extraction, concentrated by ethanol/NaOAc precipitation and purified on the Superdex 200 column using buffer N as eluent [10 mM Tris–HCl pH 7.5, 1 mM EDTA, 0.01% NP-40, 0.3 M NaCl]. Nucleosomes were then assembled by mixing the purified DNA and octamer at 1:1 molar ratio and dialyzing against buffer O [10 mM Tris–HCl pH 7.5, 1 mM EDTA, 0.01% NP-40, 0.05 M NaCl] as described in (47) and were purified by velocity sedimentation through a 15–40% sucrose gradient in buffer P [25 mM HEPES–KOH pH 7.6, 0.5 mM EDTA, 0.01% NP-40] at 192 000 × g for 20 h at 4°C using the SW-55.1 rotor. Peak fractions were dialyzed against buffer Q [10 mM Tris–HCl (pH 7.6), 1 mM EDTA, 50 mM NaCl, 0.01% NP-40]. The Cy3-labeled 6-Nuc-7 nucleosome was generated and purified similarly but the forward primer 5′-[Cy3] GCC GCC CTG GAG AAT CC-3′ was used for the PCR to generate a 6-bp linker instead of a 50-bp linker.

To prepare the H2A.Z–H2B^{FL}, H2A–H2B^{FL}, H2A.Z–H2B and H2A–H2B dimers, 2 mg of H2A, H2B, H2B^{FL} and H2A.Z proteins in buffer R [7 M guanidine–HCl, 20 mM Tris–HCl pH 7.5 and 10 mM DTT] were unfolded according to (47) and mixed at 1:1 molar ratio. The mixtures were then dialyzed against buffer M and the refolded histone dimers were purified on the Superdex 200 column in buffer M (without 2-mercaptoethanol).

In vitro histone exchange assay

The histone exchange assay was conducted using a protocol modified from (32). Each reaction is 25 μl and is composed of three parts. Part A, which constitutes 60% of the reaction volume, contains 4 nM purified SWR in 25 mM HEPES–KOH (pH 7.6), 0.5 mM EGTA, 0.1 mM EDTA, 5 mM $MgCl_2$, 0.17 μg/μl BSA, 50 mM NaCl, 10% glycerol, 0.02% NP-40. Part B, which constitutes 20% of the reaction volume, contains 75 nM Cy3-labeled AA nucleosome and 550 nM H2A.Z–H2B^{FL} dimers in 10 mM Tris–HCl (pH 7.5), 1 mM EDTA, 50 mM NaCl. Part C is 1 mM ATP and represents 20% of the reaction volume. Part A and Part B were mixed together before Part C was added to initiate the reaction. The reaction was left at room temperature (∼22°C) for the indicated times before they were quenched by the addition of 62.5 ng of lambda phage DNA (*New England Biolabs*). Five microliter of Nap1 at 3.5 μM in buffer S [70% (w/v) sucrose, 10 mM Tris–HCl (pH 7.8), 1 mM EDTA] was added to the reaction immediately before resolving the nucleosomes on 6% polyacrylamide/0.5× TBE gels. In-gel Cy3 fluorescence was detected by a Typhoon 9500 scanner (*GE Healthcare*) and densitometry was performed using the ImageQuant software. For the Swc5 rescue experiments, Swc5 and/or H2A–H2B dimer were added to the Part A and B mixture at the indicated final concentrations before adding in Part C.

ATPase assay

The ATPase assay was performed using a procedure similar to the one described in (31). The ATPase reaction is also composed of three parts but in 7:2:1 volume ratios. Part A is 2.4 nM purified SWR plus 0.7 μM phosphate sensor (fluorophore-conjugated phosphate binding protein, *ThermoFisher*) (49) in 25 mM HEPES–KOH (pH 7.6), 0.5 mM EGTA, 0.1 mM EDTA, 4.3 mM $MgCl_2$, 0.14 μg/μl BSA, 64 mM NaCl, 10% glycerol, and 0.02% NP-40. Where indicated, Part B contains 100–250 nM AA nucleosomes and 200–920 nM H2A.Z–H2B^{FL} dimers in 10 mM Tris–HCl (pH 7.5), 1 mM EDTA and 50 mM NaCl. Part C is 1 mM ATP. The reaction was initiated by the addition of Part C. Phosphate sensor fluorescence was measured at 23°C on a Biotek plate reader using the 405 nm excitation and 460 nm emission filter set at 7 sec intervals.

Binding assays for Swc5

For the binding assay between the recombinant Swc5 and the histone dimers, 0.74 μM of Swc5 was incubated with

8.7 μM of untagged H2A–H2B or H2A.Z–H2B dimers for 5 min at 4°C. The mixtures and the individual proteins were injected into the Superdex 200 10/300 Increase column at a flow rate of 0.5 ml/min using buffer T [20 mM Tris–HCl (pH 7.5), 0.3 M NaCl] as eluent. The indicated fractions in Figures 3 and 6 were precipitated by TCA before analysis by SDS-PAGE and SYPRO Ruby.

For the binding experiment of recombinant Swc5 proteins to SWR[swc5Δ], yeast extracts equivalent to 1 L of *SWR1–3xFLAG swc5Δ htz1Δ* (yEL291) culture prepared as described above were incubated with 400 μl of anti-FLAG M2 agarose beads at 4°C for 4 hours. The bead-bound SWR complexes were washed with buffer D followed by buffer E before 250 nM of recombinant Swc5 proteins were added. The mixtures were incubated with gentle shaking at 4°C for 30 min. After washing with buffer E, the SWR complexes were eluted from the beads by incubation with 0.5 μg/μl 3× FLAG peptide at 4°C for 2 h. The FLAG eluates were TCA precipitated before analysis by SDS-PAGE and SYPRO Ruby staining.

The binding experiment between SWR[swc5Δ] and the nucleosome was conducted as described in (32). For the binding experiment between the recombinant Swc5 and the AA nucleosome, nucleosomes were first assembled by mixing 14 μg of canonical yeast histone octamer with the Widom-601 sequence in the presence of 160 ng BSA and dialyzing against buffer Q. Twenty microgram of recombinant Swc5 was then added. The mixture was resolved by velocity sedimentation in a 15–40% sucrose gradient for 15 h. All fractions were TCA precipitated before analysis by SDS-PAGE and SYPRO Ruby Staining.

RESULTS

Biochemical complementation of Swc5-deficient SWR with recombinant Swc5

To investigate the molecular function of Swc5, native SWR complexes with or without Swc5 were purified from yeast extracts made from *SWR1-FLAG SWC5* and *SWR1-FLAG swc5Δ* cells, respectively, by FLAG affinity chromatography followed by glycerol gradient sedimentation (31). Consistent with previous results, the SWR complex purified from the *swc5*Δ strain (referred to as SWR[swc5Δ] hereafter) lacks only the Swc5 subunit, while the remaining 13 polypeptides exhibited the similar stoichiometry as wild-type SWR (34) (Figure 1A).

The histone exchange activity of the SWR complexes was monitored by an *in vitro* assay that allows the discrimination between the AZ and ZZ nucleosomal products (31,32). All histone substrates used in this assay were made from *S. cerevisiae* histones expressed in *Escherichia coli.* The AA nucleosomal substrate was reconstituted with the canonical histones on a 204-bp DNA fragment containing the 147-bp 'Widom-601' sequence. Optimal SWR activity requires a long linker DNA (>40 bp) on at least one side of the core particle to mimic the NFR (32). The location of the Widom-601 sequence in the 204-bp DNA is off-center resulting in the asymmetric positioning of the AA core particle such that a 50-bp linker protrudes from one side and a 7-bp linker on the other side (denoted 50-Nuc-7) (Figure 1B) (46,48). The 50-bp linker was fluorescently labeled on the 5′ end with Cy3, while the 7-bp linker was unlabeled. To distinguish between H2A–H2B and H2A.Z–H2B, the H2A.Z–H2B free dimers were assembled using H2B tagged at its C-terminus with three copies of the FLAG epitope ($H2B^{FL}$). The FLAG tag on H2B does not interfere with the SWR-mediated histone exchange reaction (31). SWR (2.4 nM) was incubated with 15 nM AA nucleosomes and 110 nM free H2A.Z–$H2B^{FL}$ dimer and the exchange reaction was initiated by the addition 200 μM ATP (the K_M of SWR for ATP is ∼5 μM) (31). At various times, the reaction was quenched by the addition of excess lambda phage DNA and the mobility of the nucleosomes was analyzed by native polyacrylamide gel electrophoresis (PAGE) to determine their histone composition. The histone chaperone Nap1 was added to all reaction after quenching but immediately before the native PAGE analysis to prevent non-specific binding of any free H2A.Z–$H2B^{FL}$ dimers to the nucleosomes (Supplementary Figure S2A, and compare lanes 1 and 3 in S2B).

The replacement of the untagged nucleosomal H2A–H2B with H2A.Z–$H2B^{FL}$ decreased the mobility of the nucleosome in native PAGE in an additive manner. As such, the mobility of the AZ nucleosome with one H2A.Z–$H2B^{FL}$ is slower than the untagged AA nucleosome but faster than the ZZ nucleosome, which has two H2A.Z–$H2B^{FL}$ dimers (Figure 1B and C). The progress of the reaction was quantified by the in-gel Cy3 florescence [or SYBR Green staining (below)] of the nucleosomal DNA (Figure 1D). As expected, SWR converts the AA nucleosome to the AZ and ZZ species in a stepwise manner at a rate similar to previously published results (31,32).

Nap1 can exchange H2A.Z–H2B (or H2A–H2B) into nucleosomes in an ATP-independent manner (50), raising the possibility that Nap1 contributes to the formation of the AZ and ZZ nucleosome, instead of SWR. This caveat was eliminated by showing that reactions with or without Nap1 had no effect on the mobility of the nucleosomal products (Supplementary Figure S2B and D, compare lanes 2 and 4). In fact, even when the quenched SWR reaction was allowed to incubate with Nap1 for 1 h, no further exchange of H2A.Z–$H2B^{FL}$ into the nucleosomes was detected (Supplementary Figure S2B, compare lanes 2 and 6). Therefore, the mobility shift of the nucleosome in the native gel assay is directly caused by the ATP-dependent histone exchange activity of SWR.

The heterotypic AZ (or ZA) species appears as a doublet in the native gel (Figure 1C). This mobility difference could be due to the two possible sites that H2A.Z–$H2B^{FL}$ can be incorporated relative to the longer linker of the asymmetrically positioned nucleosome (Figure 1B). This idea was confirmed using a nearly symmetrical nucleosome substrate with 6-bp and 7-bp linkers on either side (6-Nuc-7). When SWR was incubated with the 6-Nuc-7 substrate, only one type of AZ intermediate was observed (Figure 1E).

The SWR[swc5Δ] complex exhibited virtually no detectable histone exchange activity (Figure 1F and G, Supplementary Figure S3). Addition of recombinant yeast Swc5 protein partially restored the activity of SWR[swc5Δ], indicating that Swc5 can be inserted into the pre-folded SWR[swc5Δ] complex (Figure 1H and I). It should be

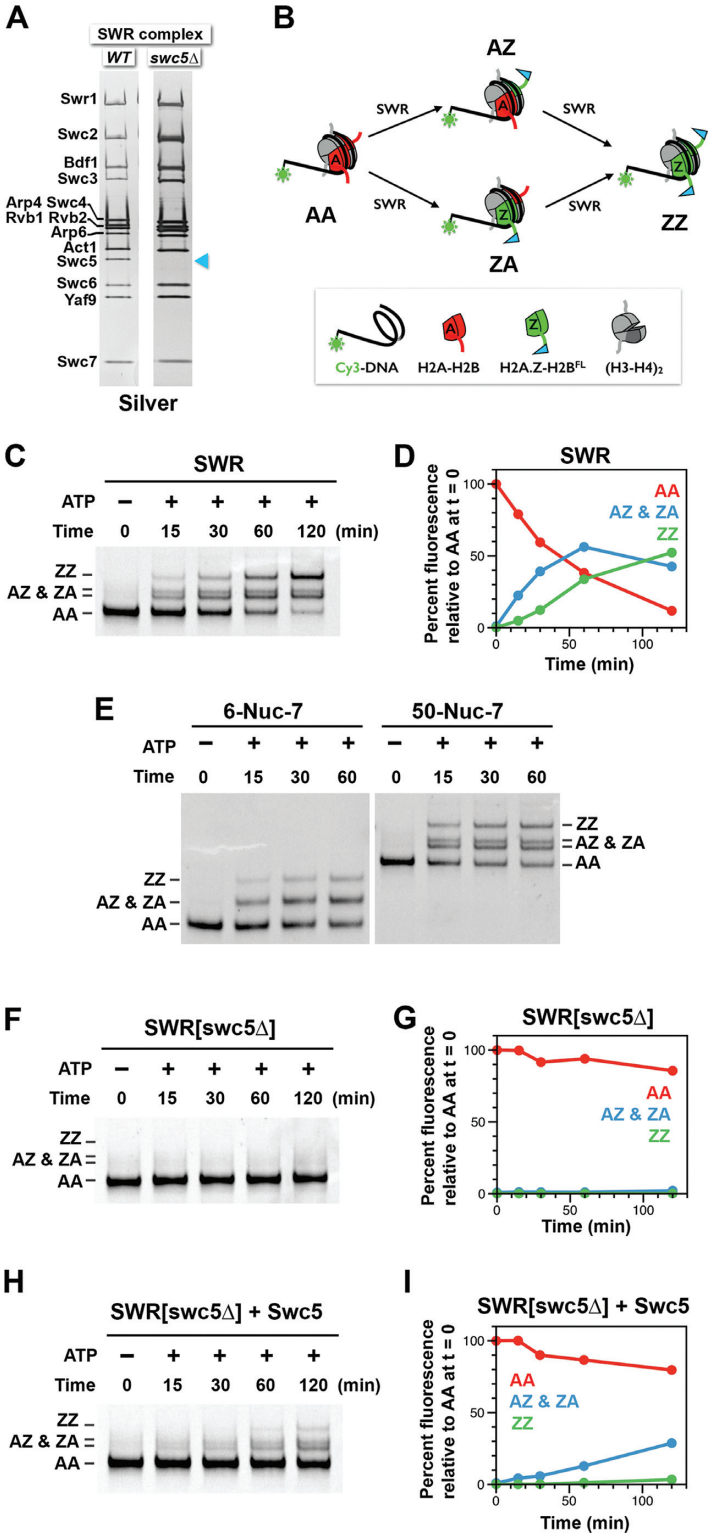

Figure 1. Recombinant Swc5 complemented the histone exchange activity of SWR[swc5Δ] in vitro. (**A**) The SWR complexes from wild-type and *swc5Δ* yeast were analyzed by SDS-PAGE and silver staining. The cyan arrowhead indicates the position of Swc5. (**B**) A cartoon depicting the structural organization of the AA nucleosomal substrate, the AZ and ZA intermediates, and the ZZ product. (**C**) *In vitro* histone exchange of wild-type SWR. The nucleosomal species before and after the addition of ATP were resolved on a native 6% polyacrylamide gel (0.5x TBE) and scanned to reveal Cy3 fluorescence. (**D**) Quantification of the AA, (AZ+ZA), and ZZ nucleosome bands in (**C**) as a function of reaction time. (**E**) *In vitro* histone exchange using the nucleosomal substrate 6-Nuc-7 on *left* or 50-Nuc-7 on *right*. The *left* and *right* panels were cropped from the same gel. The extra 44 bp of DNA in the 50-Nuc-7 as compared to 6-Nuc-7 increased the overall mobility of the AA, AZ and ZZ species. (**F** and **G**) *In vitro* histone exchange of SWR[swc5Δ] histone exchange reaction was conducted as described in **C**. (**H** and **I**) Same as F and G, except that recombinant Swc5 was added to the reaction before the addition of ATP.

noted that ∼60-fold excess of Swc5 (150 nM) relative to SWR[swc5Δ] was used in this rescue experiment; however, a similar level of rescue was obtained when stoichiometric amount of Swc5 was used (see below).

Swc5 is required for the stimulation of SWR ATPase

To understand how Swc5 is involved in H2A.Z deposition, we investigated the requirement of Swc5 for SWR ATPase stimulation in response to substrate binding. The activity of the SWR ATPase was indirectly monitored by the Phosphate Sensor protein, which increases in fluorescence when bound to the phosphate released during ATP hydrolysis (49). As expected, wild-type SWR was partially stimulated by AA nucleosomes and hyper-stimulated by both AA nucleosomes and H2A.Z–H2B dimers (Figure 2A and B) (31). By contrast, the stimulation of the ATPase of SWR[swc5Δ] in response to the histone substrates was severely impaired, although the basal activity remains similar to that of wild-type SWR (Figure 2A and B). The addition of recombinant Swc5 was able to partially rescue the ATPase response of SWR[swc5Δ], indicating that Swc5 is responsible for the stimulation of the SWR ATPase in response to the binding of its histone substrates (Figure 2C and D).

Swc5 is not required for SWR binding to its substrates

One explanation for the decreased ATPase stimulation of SWR[swc5Δ] is that Swc5 is required for optimal binding of either the AA nucleosome, the H2A.Z–H2B dimer, or ATP. To test if SWR[swc5Δ] is defective in binding the AA nucleosome, wild-type SWR and SWR[swc5Δ] complexes were incubated with fluorescently labeled AA nucleosomes. SWR-bound nucleosomes were then separated from unbound nucleosomes by native agarose electrophoresis. SWR[swc5Δ] was bound to H2A nucleosomes to a similar degree as the wild-type SWR, consistent with an earlier result (Supplementary Figure S4) (32). However, this experiment does not rule out subtle defects in SWR[swc5Δ] binding to AA nucleosomes that may be revealed under the reaction conditions of the ATPase assay. To test this possibility, SWR[swc5Δ] ATPase activity was measured as a function of increasing AA nucleosome concentration in the presence of excess H2A.Z–H2B and ATP. If the binding of AA nucleosome to SWR[swc5Δ] is suboptimal, increasing the nucleosome concentration could compensate for the binding defect and restore the ATPase stimulation. However, the ATPase activity of SWR[swc5Δ] remained unchanged in response to increasing nucleosome concentrations, suggesting that the low ATPase stimulation is not due to defective nucleosome binding (Supplementary Figure S5A).

A similar approach was used to evaluate whether SWR[swc5Δ] is defective in binding H2A.Z–H2B dimers or ATP. No increase of ATPase activity in SWR[swc5Δ] was observed at increased H2A.Z–H2B dimer or ATP concentrations while the other two substrates were held constant in excess (Supplementary Figure S5B and S5C). Altogether, our data argue against the role of Swc5 in substrate binding. Rather, Swc5 appears to be required to communicate the recognition of the histone substrates to the ATPase to allow optimal stimulation.

Swc5 binds to the H2A–H2B dimer—a remodeling product of SWR

Although Swc5 does not bind to the substrates of the histone exchange reaction, this does not rule out the possibility that it may function by binding to the products of the reaction, for example, the H2A–H2B dimers that are removed from the nucleosomes. This potential interaction was evaluated using a biochemical approach (Figure 3A–D). Recombinant Swc5 was mixed with either untagged H2A.Z–H2B (Z-B) or H2A–H2B (A–B) dimers *in vitro* and analyzed for the complex formation by size exclusion chromatography where the ternary complexes would flow more quickly through the column. Swc5 and H2A.Z–H2B dimer do not interact under the experimental conditions as the two species migrated independently as if they were injected individually into the gel filtration column (Figure 3A and B). By contrast, when Swc5 and H2A–H2B dimer were co-injected into the column, a faster migrating complex corresponding to the Swc5•[H2A–H2B] complex was observed [Figure 3C and D, Swc5•(A-B)]. In a separate experiment, stable Swc5•[H2A–H2B] complex was similarly detected when recombinant Swc5, H2A, and H2B polypeptides were refolded by dialysis and then analyzed by gel filtration (Supplementary Figure S6). Since H2A–H2B dimer is a product of the histone replacement reaction, the preferential binding of Swc5 to H2A–H2B implies that Swc5 may facilitate the histone exchange process by stabilizing the histone ejection step.

To further understand the functional importance of the interaction between Swc5 and H2A–H2B, excess free H2A–H2B dimers were used to block the putative H2A–H2B binding site of Swc5 within SWR in an attempt to inhibit the histone exchange reaction *in vitro*. As expected, a reduction in the formation of AZ and ZZ nucleosomes was observed when excess H2A–H2B dimers were present (Figure 3E, compare lanes 2 and 6). Next, we used free Swc5 as a histone chaperone to relieve the inhibitory effect of the excess H2A–H2B dimers in *trans*. When equimolar amounts of free Swc5 and H2A–H2B were added, the ability of SWR to incorporate H2A.Z–H2B was partially restored (Figure 3E, compare lanes 6 and 8). The incorporation of H2A.Z–H2B was increased further when even more Swc5 was used (Figure 3E, compare lanes 8 and 10). Nap1, which binds both H2A–H2B and H2A.Z–H2B (29,50), was ineffective in relieving the H2A–H2B inhibition (Figure 3F, compare lanes 4, 6 and 8).

One possible role of Swc5 is that it acts as an evictor of H2A–H2B during the histone exchange process. Alternatively, Swc5 may function as a gatekeeper to prevent the misincorporation of H2A–H2B into the AA nucleosome. However, since both the free and nucleosomal H2A–H2B dimers were untagged, we cannot tell if the diminished H2A.Z–H2B^{FL} insertion was caused by competitive H2A–H2B misincorporation or by inhibition of the directional H2A-to-H2A.Z exchange (Figure 3E, lane 6). To distinguish between these possibilities, excess H2A–H2B^{FL} (i.e. with a 3xFLAG tag on H2B) was used to assess the degree of H2A–H2B misincorporation (Figure 3G). The results showed the level of H2A–H2B^{FL} misincorporation was insignificant, arguing against competitive inhibition by H2A–

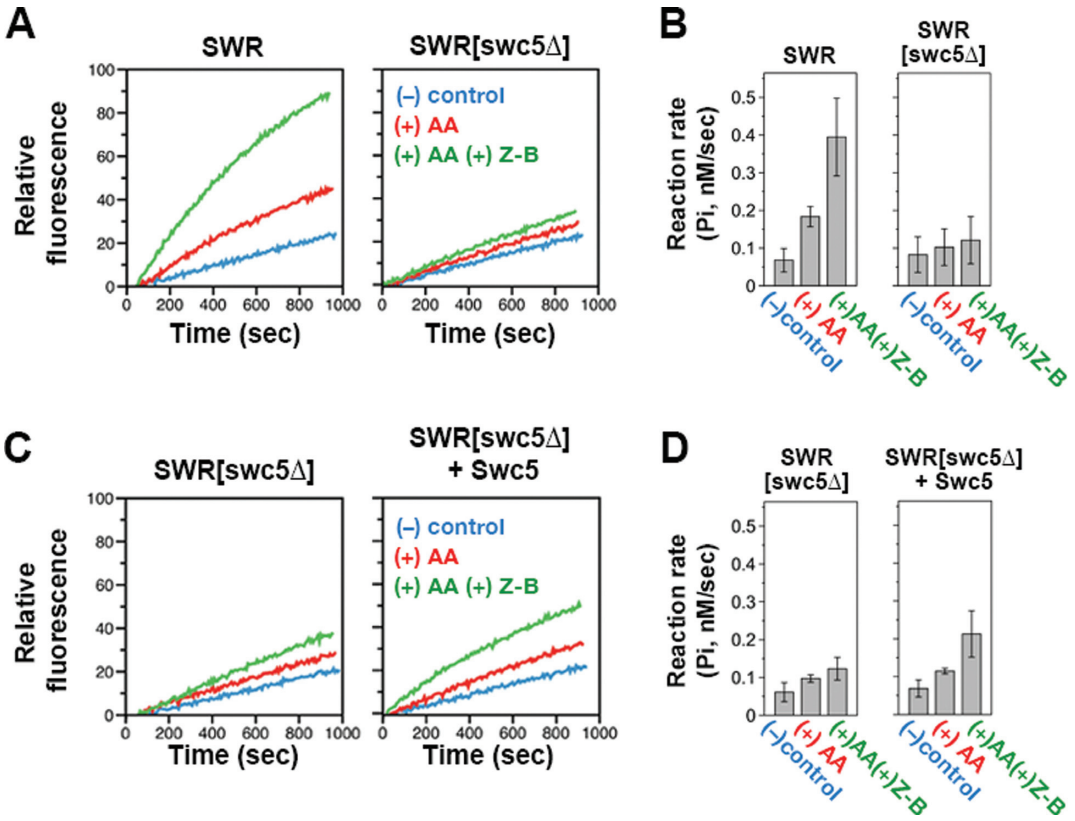

Figure 2. Swc5 is required for SWR ATPase activation. (**A**) *Left panel:* The ATPase activity of wild-type SWR (1.2 nM) in the presence or absence of AA nucleosomes (20 nM) and H2A.Z–H2B^{FL} (Z-B) dimers (40 nM). *Blue*: enzyme alone control; *red*: enzyme plus H2A nucleosome; *green*: enzyme plus H2A nucleosome and H2A.Z–H2B dimer. *Right panel:* Same as the *left*, except that the mutant SWR[swc5Δ] was used. (**B**) Initial rates were calculated based on the averages of three independent reactions for each enzyme in (A). Error bars represent the standard deviation. (**C**) ATPase activities of SWR[swc5Δ] alone (*left*) and SWR[swc5Δ] plus recombinant Swc5 (*right*). It is necessary to repeat the ATPase assay for the SWR[swc5Δ] alone control since the reaction buffer composition was different from (A) when recombinant Swc5 was added to the reaction. (**D**) Quantification of the reactions of (C) as in (A).

H2B misincorporation. Rather, our data suggest that the Swc5 subunit of SWR functions as a specific H2A–H2B chaperone in assisting the eviction step of the histone exchange reaction.

The conserved BCNT domain of Swc5 is required for H2A.Z deposition

Swc5 is conserved from yeast to humans (Supplementary Figure S7). Yeast Swc5 is a 303-amino-acid (aa) protein. Informatics predicts that over half of the polypeptide sequence on the N-terminal side is disordered (based on PrDOS), interrupted mainly by two short (∼15–35 aa) structural elements (Supplementary Figure S7A) (51). Twenty-five of the first 54 residues in the disordered N-terminus are the negatively charged aspartate and glutamate residues, thus averaging a pI of <4 within this region (Figure 4A, and Supplementary Figure S7A, D/E domain). By contrast, the C-terminal end starting from residue 234 of the yeast protein is associated with strong alpha helical characteristics (based on Phyre2) (52). This region overlaps a highly conserved domain called Bucentaur or BCNT (Pfam: PF07572) (Figure 4A and Supplementary Figure S7A).

To understand how these different regions of Swc5 are involved in H2A.Z deposition, mutants of *SWC5* were tested for their ability to complement *swc5Δ* yeast. Cells defective for SWR-mediated H2A.Z deposition are sensitive to formamide (19). As expected, *swc5Δ* yeast failed to grow on formamide (Figure 4B). This growth defect was rescued by a single-copy episomal plasmid containing *SWC5* (Figure 4B). To determine whether the BCNT domain is important for Swc5 function, alleles encoding truncations of the Swc5 C-terminus were constructed: *swc5 (1–254*)* and *swc5 (1–232*)*, where asterisks indicate stop codons. Both *swc5 (1–254*)* and *swc5 (1–232*)* failed to complement *swc5Δ* for growth on formamide (Figure 4B). To determine the functional significance of two highly conserved motifs near the N-terminal side of the BCNT domain, TTLEKS and LDW, these motifs were mutated to alanines. Both the *swc5(TTLEKS→6A)* and *swc5(LDW→3A)* failed to complement, indicating that at least one of the amino acids in each domain is essential for *SWC5* function (Figure 4C-D). By contrast, an allele substituting the semi-conserved FAGE motif within the 35-aa structural element with alanines complemented almost the same as *SWC5* (Figure 4D). The conserved acidic D/E domain at the N-terminus is not required for *SWC5* function as the *swc5 (79–303)* mutant was capable for rescuing *swc5Δ* (Figure 4C). But when the N-terminus was truncated further to position 146, the resulting *swc5 (147–303)* mutant was no longer functional (Figure 4C).

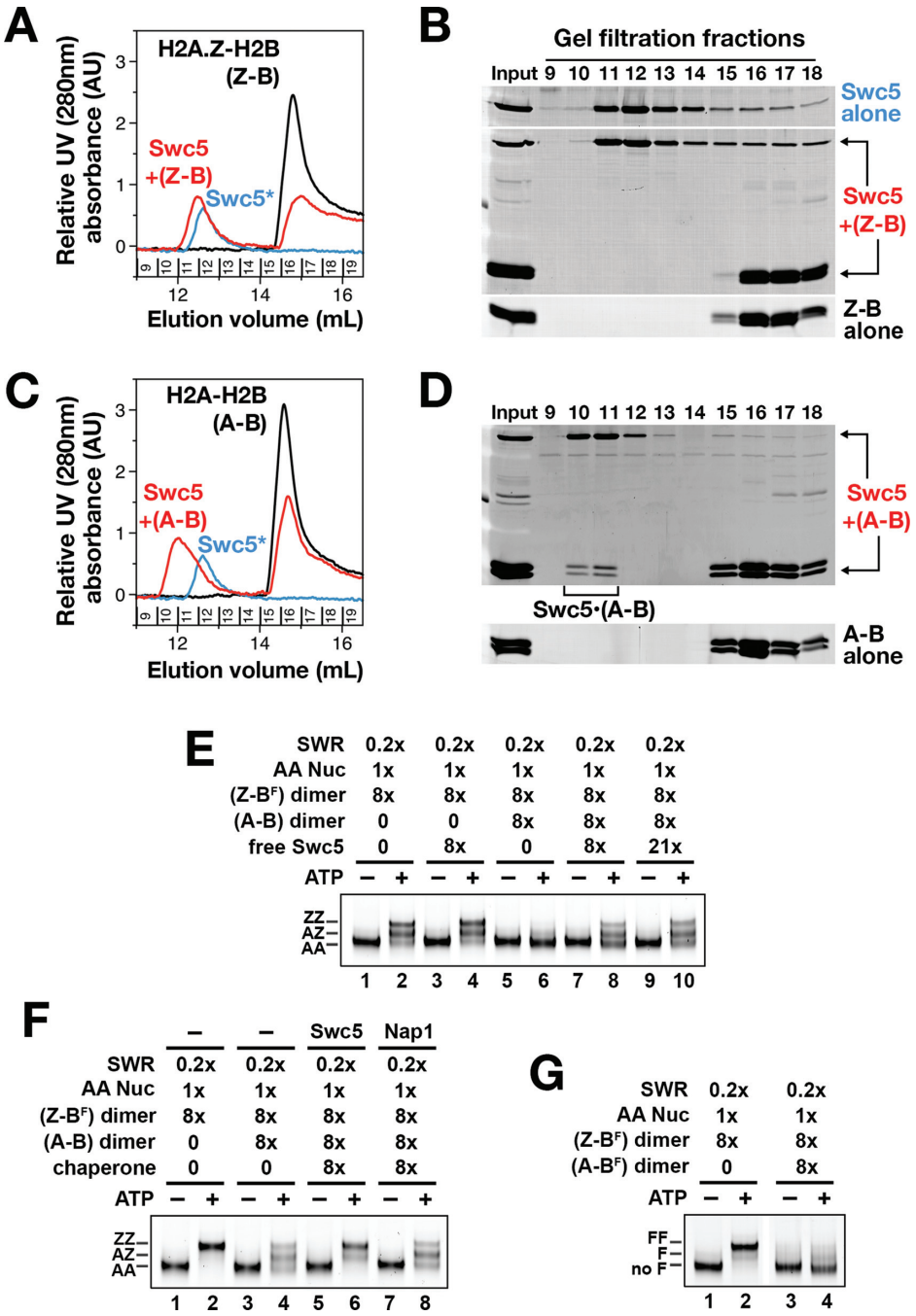

Figure 3. Swc5 forms a complex with H2A–H2B, but not H2A.Z–H2B. (**A** and **B**) Gel filtration elution profiles of the H2A.Z–H2B (Z-B) dimer alone (*black*), Swc5 protein alone (*blue*), and Swc5 mixed with Z-B (*red*). The numbers oriented vertically correspond to the chromatographic fractions indicated in (B), which shows the SDS-PAGE analysis of the chromatographic fractions. (**C**) Gel filtration profiles of the H2A–H2B (A–B) dimer alone and Swc5 plus A-B. Asterisk indicates that the same Swc5 profile was used for both (A) and (B). (**D**) SDS-PAGE analysis of (C). SYPRO Ruby was used to stain the proteins in (B) and (D). (**E**) SWR-mediated histone exchange in the presence or absence of excess H2A–H2B and/or free Swc5. The initial substrate concentration of H2A nucleosomes (Nuc) was 15 nM, which was defined as 1×. (**F**) Same as E, except that Swc5 was replaced by Nap1 in lanes 7 and 8. (**G**) Same as E, except that H2A–H2B^{FL} (A–B^{F}) was used. FF, nucleosomes with two FLAG tags; F, with one FLAG tag; no F, with no FLAG.

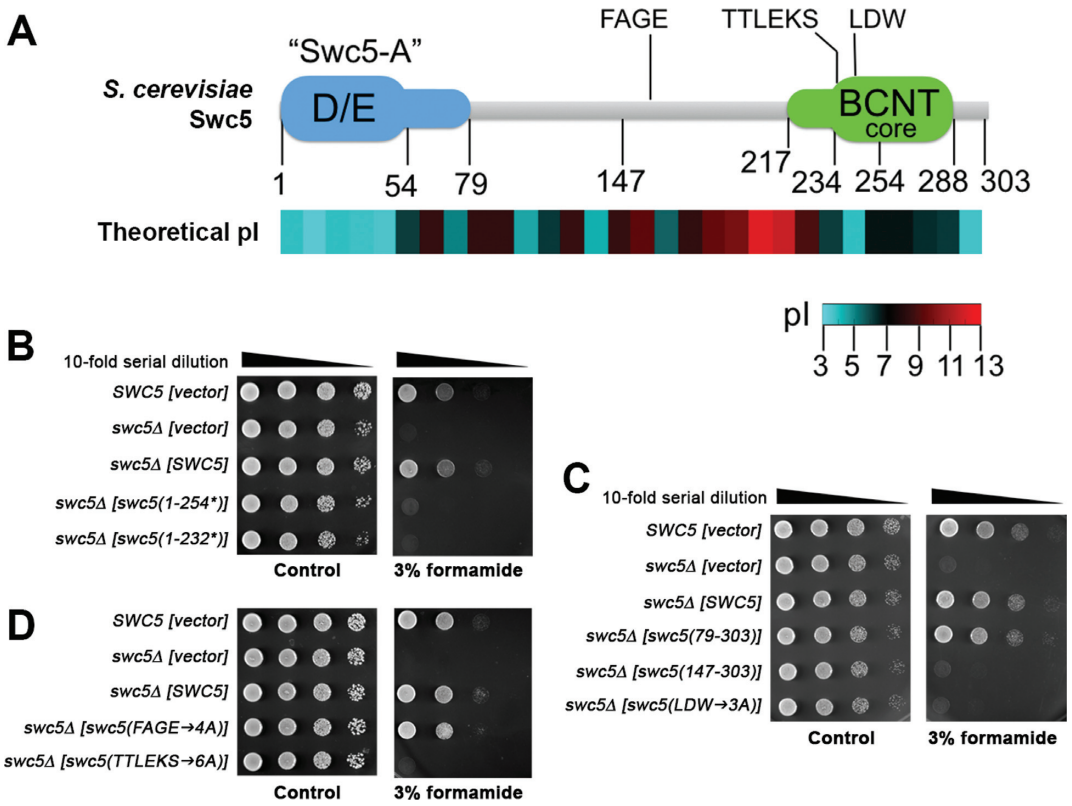

Figure 4. Domain analysis of Swc5 by genetic complementation. (**A**) A cartoon representation of Swc5 highlighting the conserved domains and motifs, as well as amino acid positions relevant to the domain analysis. The heatmap below represents the theoretical pI calculated from a moving window of 20 amino acids (aa) at a resolution of 10 aa. (**B–D**) Formamide sensitivity of various *swc5* mutants. The *swc5Δ* haploid (yEL274) was transformed with *URA3 CEN ARS* plasmids containing various alleles of *SWC5* under the control of the endogenous *SWC5* promoter. The *SWC5* haploid (BY4741) transformed with the *URA3* vector was included as a control. Plasmid genotypes are written in brackets.

The inability of the BCNT domain mutants to complement the phenotype of *swc5Δ* could be indirect. For example, the BCNT domain may be required for protein folding or stability *in vivo*. Western analysis of whole cell extracts using a polyclonal antibody raised against the full length Swc5 showed the protein levels of swc5(TTLEKS→6A) and swc5(LDW→3A) were similar to wild type arguing against protein instability being the reason for the failure of these mutant to complement *swc5*Δ (Supplementary Figure S8). Because truncation of Swc5 may remove epitopes resulting in an artifactual reduction of signal on immunoblots, these mutants were not included. To further confirm whether BCNT domain has a direct role in the chromatin remodeling function of SWR, Swc5 protein and its mutant derivatives were purified from *E. coli* and added back individually to the histone exchange reactions. Stoichiometric amounts of wild-type or mutant Swc5 proteins (2.5 nM) were test for their ability to restore the activity of SWR[swc5Δ] (2.5 nM) *in vitro* (Figure 5A–D). A good correlation was observed between the ability to generate the AZ and ZZ nucleosomes and growth on formamide (Figures 4B–D and 5C–D). None of the mutants of the BCNT domain [i.e. swc5 (1–254*), swc5 (1–232*), swc5(TTLKES→6A), and swc5(LDW→3A)] were able to rescue SWR[swc5Δ] (Figure 5C and D).

One explanation for the loss of function in the BCNT domain mutants is that this region of Swc5 mediates the interaction with SWR. To test this possibility, SWR[swc5Δ] was immobilized on anti-FLAG beads and was incubated with an excess amount of wild-type Swc5 or the swc5 (1–232*) mutant. The complexes were then liberated from the beads by FLAG peptide elution and analyzed by SDS-PAGE and SYPRO Ruby staining to detect the proteins (Figure 5E, compare lanes 2 and 3). Stoichiometric amounts of Swc5 and the BCNT truncated swc5 (1–232*) co-eluted with the components of the SWR[swc5Δ] complex, indicating that the core region of the BCNT domain (Supplementary Figure S7) is not required for binding SWR but is likely involved in some mechanistic steps during the histone exchange reaction.

It should be noted that the recombinant Swc5 has a larger molecular weight than the native Swc5 (Figure 5E, compare lanes 2 and 5). This was due to the presence of the epitope tag at the N-terminus of Swc5. The tag did not interfere with SWR activity as removing the tag by thrombin cleavage did not enhance Swc5′s ability in rescuing SWR[swc5Δ] (Supplementary Figure S9).

The acidic N-terminal domain of Swc5 enhances SWR activity by preferentially binding to the H2A–H2B dimer

In vivo, the N-terminal D/E domain truncation mutant *swc5 (79–303)* complements the *swc5Δ* cells to a similar level as *SWC5* (Figure 4C). However, the rescue of the *in*

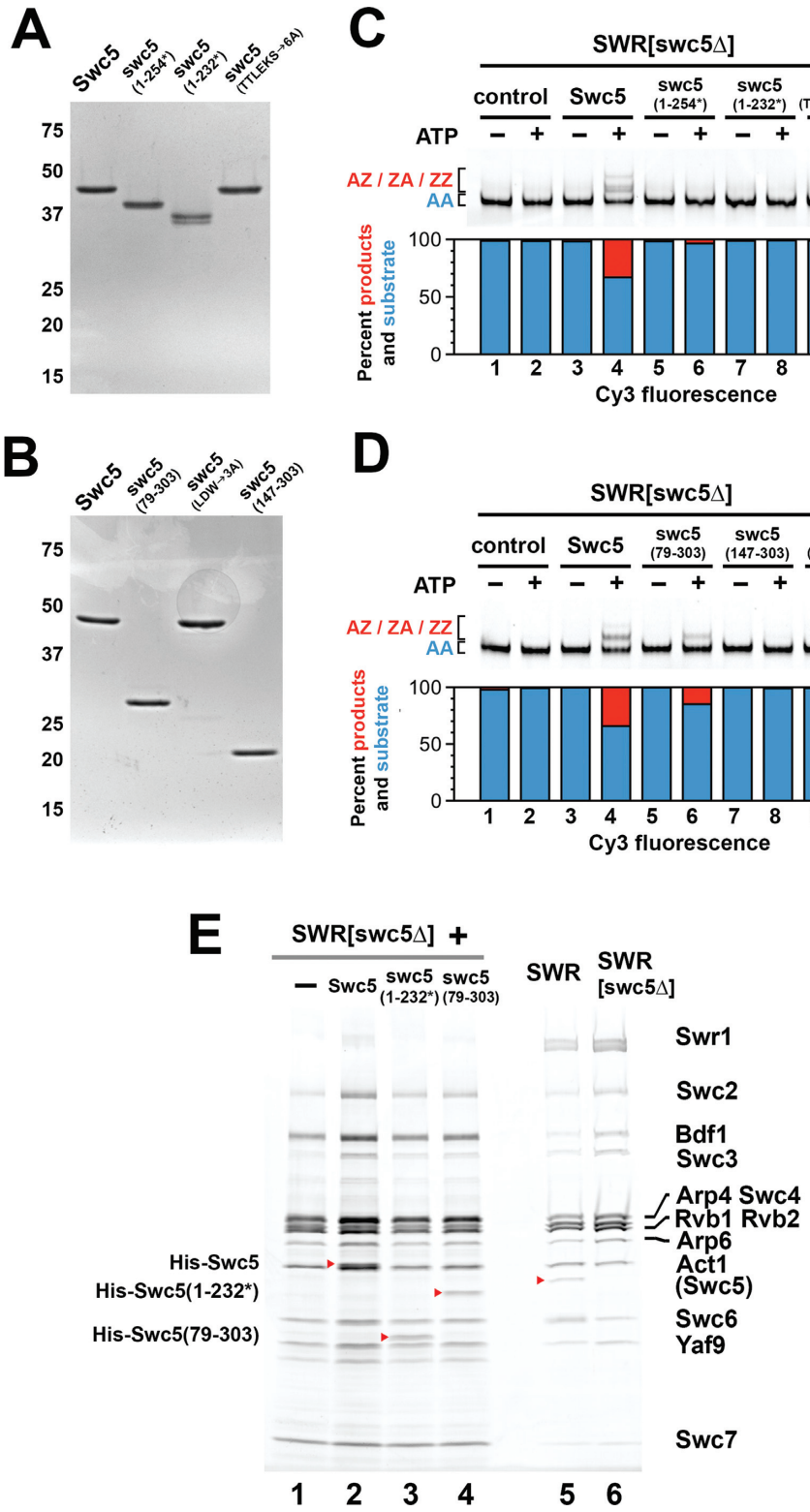

Figure 5. Domain analysis of Swc5 by complementation of SWR[swc5Δ] activity in vitro. (**A** and **B**) Recombinant yeast Swc5 and mutant variants and were analyzed by SDS-PAGE and SYPRO Ruby staining. (**C** and **D**) Histone exchange activity of SWR[swc5Δ] was assayed as described in Figure 1H but in the presence or absence of 2.5 nM purified Swc5 and mutant variants (i.e. equimolar relative to SWR[swc5Δ]). The band intensity corresponding to the AA nucleosome (*blue*) and the combined intensities for the AZ/ZA/ZZ products (*red*) were quantified in the bottom panel. (**E**) *Lanes 1–4*: SDS-PAGE analysis and SYPRO Ruby staining of Swc5 and its mutant variants that co-eluted with the SWR[swc5Δ] complex. *Red* arrowheads indicate the position of the recombinant Swc5 protein bands. *Lane 5–6*: Purified wild-type SWR and SWR[swc5Δ] were loaded in the same gel for comparison.

vitro histone exchange activity of SWR[swc5Δ] is only partial when the swc5 (79–303) protein was used (Figure 5D, compare lanes 4 and 6). This result suggests that the D/E domain of Swc5 is required for optimal chromatin remodeling activity. Since proteins with acidic domains are known to bind to free histones (53), we hypothesized that the D/E domain is responsible for the preferential binding of the H2A–H2B dimer as seen in Figure 3C-D. To test this, recombinant H2A–H2B was incubated with swc5 (79–303) followed by injection into the gel filtration column. Without the acidic D/E domain, no ternary complex between swc5 (79–303) and H2A–H2B was formed (Figure 6A and B). By contrast, the swc5 (1–232*) mutant, which lacks the C-terminal BCNT domain, formed a higher molecular weight complex with H2A–H2B [labeled as swc5 (1–232*)•(A-B) in Figure 6C and D], indicating that the BCNT domain is not required for H2A–H2B binding. These results support the idea that the acidic N-terminal D/E domain, called the Swc5-A domain hereafter (conforming with the nomenclature of the histone binding domains of SWR), is required for binding to the H2A–H2B dimer.

Since SWR[swc5Δ] is capable of binding to the AA nucleosome, the fact that Swc5 can bind to the H2A–H2B dimer raises the possibility that the subunit contributes to the binding of the nucleosome substrate. To test this, Swc5 was incubated with the AA nucleosome and the mixture was then separated on a sucrose gradient. No apparent interaction was observed between Swc5 and the AA nucleosome (Supplementary Figure S10).

To test if Swc5-A domain is required for relieving the inhibitory effect of excess H2A–H2B on SWR activity, the purified swc5 (79–303) was added to the *in vitro* histone exchange reaction that was inhibited by excess H2A–H2B. As seen in Figure 6E, swc5 (79–303) did not improve the formation of AZ and ZZ nucleosomes relative to the control without free Swc5 (Figure 6E, compare lanes 4, 6 and 10). By contrast, the BCNT truncation mutant swc5 (1–232*), which contains the intact Swc5-A domain, was able to partially relieve the inhibitory effect of the free H2A–H2B dimers (Figure 6E, compare lanes 4, 6 and 8). These findings support the idea that the interaction between Swc5-A and H2A–H2B is functionally important for the SWR-mediated histone exchange reaction.

DISCUSSION

Proposed mechanisms on how Swc5 couples substrate recognition to ATPase stimulation

Swc5 is essential for SWR-mediated H2A.Z deposition *in vitro* and *in vivo*, but how this subunit participates in the histone exchange mechanism was unclear (25,34). This work shows that Swc5 is required for optimal stimulation of the SWR ATPase when the remodeler is bound to the *in vivo* histone substrates, i.e. H2A-containing nucleosomes and H2A.Z–H2B dimers (Figure 7, symbolized by the *orange arrows*). The next question is how Swc5 stimulates the SWR ATPase at the mechanistic level. One possibility is that Swc5 may function as a linchpin that holds the Swr1 polypeptide scaffold in a conformation that is capable to be activated. Alternatively, but not exclusively, Swc5 may act as a molecular lever that transduces the conformational change caused by the binding of the histone substrates to a regulatory component of Swr1 ATPase to lift its inhibition.

Crosslinking analysis of native SWR followed by mass spectrometry revealed proximity of Swc5 to the Swr1 polypeptide at regions near the ATPase domain and the HSA domain, which has been implicated in ATPase regulation (33,54). Biochemical studies further showed that stable interaction of Swc5 to the SWR complex requires two regions flanking the Swr1 ATPase domain: a 17-aa region at the C-terminus of Swr1 and a region immediately downstream of the HSA domain called the post-HSA domain (44,54). In the RSC remodeler complex, the HSA domain, which serves as a platform for the assembly of the actin-related proteins Arp7 and Arp9, and Rtt102, together with the post-HSA domain, couple ATPase activity to histone movement (54,55). Similar regulatory function may be exerted by the Swr1 HSA and post-HSA domains and its associating factors actin (Act1) and Arp4 (54,56) (Figure 7). A recent study showed Swc5 is physically linked to one of two actin subunits within SWR (44), suggesting that this actin could be working together with Swc5 to regulate ATPase motor activity.

Interestingly, the same study also showed SWR without Swc5 exhibits normal ATPase stimulation when bound by AA nucleosomes, in contrast to our results (44). The cause of the discrepancy is unknown but could be due to the different sources of SWR used in the *in vitro* assays. Our SWR[swc5Δ] complex was purified from yeast and may contain native post-translational modification(s) that suppress substrate-dependent ATPase activation when Swc5 is absent. The yeast SWR[swc5Δ] complex purified by Lin *et al*. was expressed in insect cells and may lack such regulatory modification(s) (44).

Activation of the SWR ATPase also requires the Swc2 subunit (57). SWR purified from *swc2Δ* cells lacks Swc2 and Swc3 and is deficient for the Swc6, and Arp6 subunits (32,34). The resulting SWR[swc2Δ] complex has no histone exchange activity and the SWR ATPase cannot be activated by the histone substrates (57). However, unlike SWR[swc5Δ], the SWR[swc2Δ] complex has strong defects in the binding of AA nucleosomes and H2A.Z–H2B dimers (32,34). This binding defect could be the basis for the loss of ATPase activation in SWR[swc2Δ].

Incubating recombinant Swc5 with native SWR[swc5Δ] purified from yeast restored the H2A.Z deposition activity of the complex *in vitro*. This result suggests that Swc5 binds to the SWR complex at a location that is solvent accessible. However, the rescue of the histone exchange activity was partial even when recombinant Swc5 was bound to the SWR complex stoichiometrically. One explanation could be that Swc5 is covalently modified *in vivo* to allow optimal activation of SWR. Consistent with this idea, mass spectrometry studies have identified phosphorylation sites in the yeast Swc5 and the human CFDP1 homolog (58,59). Alternatively, but not exclusively, Swc5 may be important to stabilize the rest of the SWR components. In the absence of Swc5, some critical components of SWR may have dissociated irreversibly after purification, preventing the partial complexes from being rescued by the recombinant Swc5.

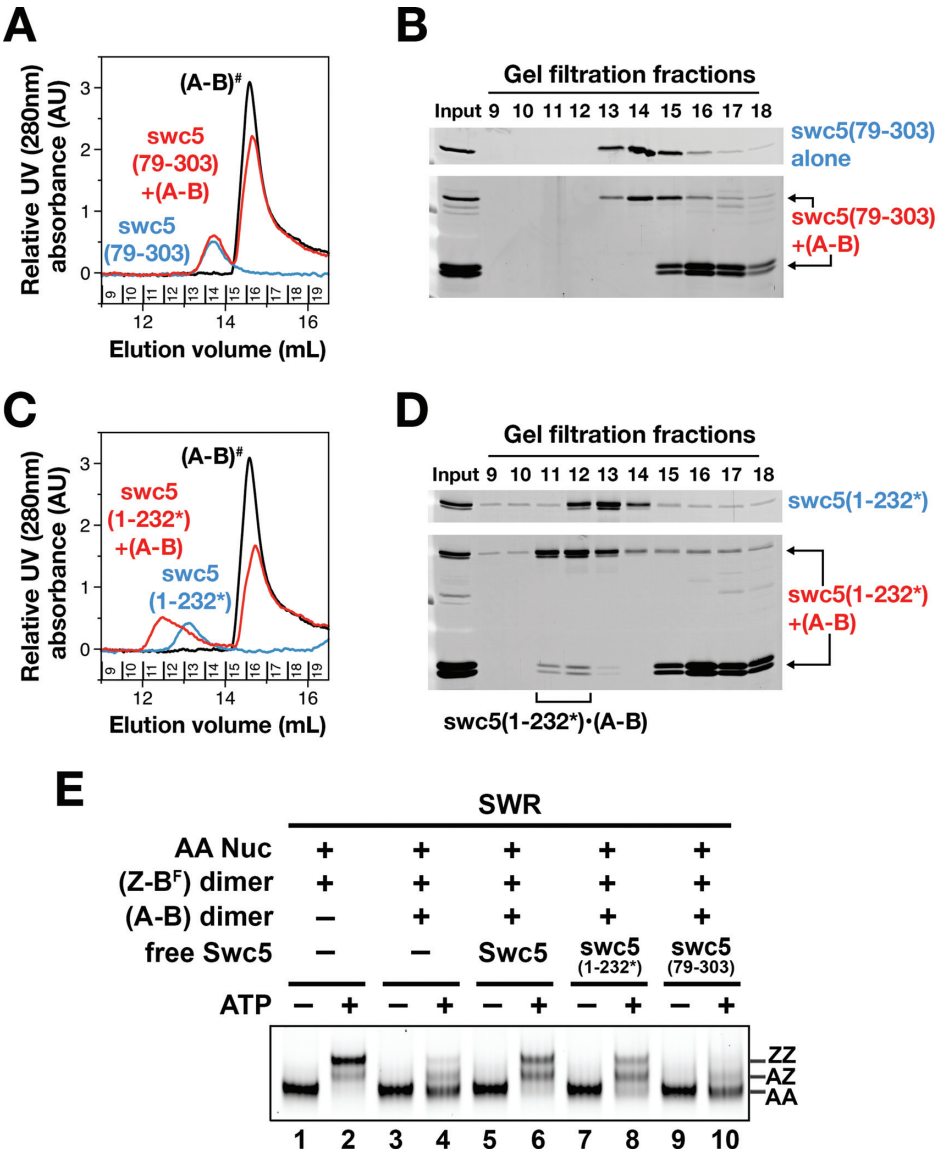

Figure 6. The acidic Swc5-A domain is required for H2A–H2B binding. (**A** and **C**) Gel filtration profiles of H2A–H2B (A-B) alone (*black*), swc5 truncation mutant proteins alone (*blue*), or the Swc5 mutant proteins mixed with A-B dimers (*red*). **B** and **D** are the SDS-PAGE analysis of the corresponding fractions in **A** and **C**, respectively. Gel filtration runs were performed as described in Figure 3. The # sign indicates that the H2A–H2B elution profile from Figure 3C was re-plotted in **A** and **C** as reference. (**E**) SWR-mediated histone exchange in the presence of excess H2A–H2B and in the presence or absence of Swc5 or its mutant variants. The reaction conditions are the same as Figure 3E.

The conserved Swc5-A domain is required for specific H2A–H2B binding

An outstanding question in the understanding of SWR-mediated histone exchange reaction is whether the remodeler assists in the eviction of the H2A–H2B dimer (9). Our work has uncovered a previously unknown function of Swc5—the preferential binding to the H2A–H2B dimer to assist its eviction during the histone exchange process. The binding specificity of Swc5 for H2A as a free dimer with H2B rather than H2A in the context of the nucleosome suggests that Swc5 recognizes at least part of the surface on the H2A–H2B dimer that is excluded by the DNA or the other histones within a nucleosome. The Swc5-A domain is predicted to be unstructured, suggesting that induced folding is expected upon binding to the H2A–H2B dimer. Similar examples have been documented for several histone binding domains, including the Chz-domain of Chz1, the Swr1-Z domain of Swr1, and the Swc2-Z domain of Swc2 (42,60,61). But unlike the aforementioned examples, where the H2A.Z–H2B dimer is the preferred binding partner, the Swc5-A domain of Swc5 prefers H2A–H2B.

Although the Swc5-A domain is required for optimal H2A.Z deposition *in vitro*, it is dispensable *in vivo* based on the formamide plate test, which is a proxy for *in vivo* H2A.Z deposition. One explanation for this discrepancy is that the *in vitro* exchange assay is more sensitive and thus is capable of revealing the partial H2A.Z deposition defect of the Swc5-A domain truncation mutant, whereas the formamide test can tolerate the suboptimal deposition of H2A.Z. Al-

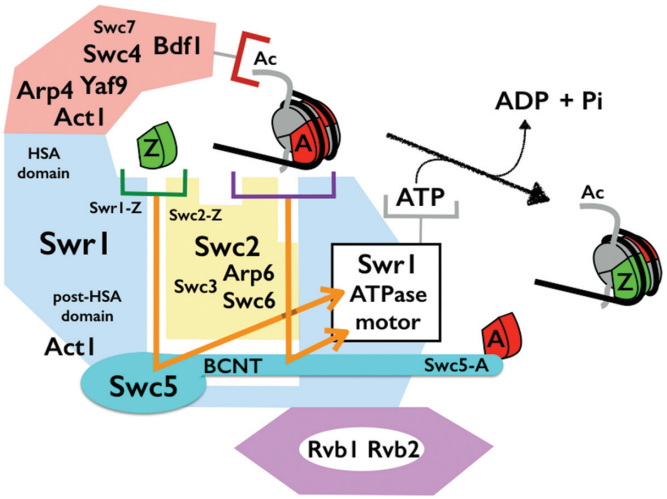

Figure 7. A cartoon highlighting the molecular role of Swc5 in the SWR-mediate histone exchange reaction. Half brackets: binding sites for AA nucleosome (*purple*), histone tail modifications (*red*), H2A.Z–H2B (*green*), and ATP (*gray*). The binding of SWR to its substrates involves the Swc2 and Swr1 subunits (depicted by the overlaps between the yellow/blue regions and the brackets). The Swc2-Z domain binds H2A.Z–H2B and a basic region in Swc2 binds the NFR next to the +1 nucleosome. The Swr1-Z domain contributes to the binding of H2A.Z–H2B. Swc5 couples substrate recognition to the activation of the SWR ATPase (*orange arrows*). The acidic Swc5-A domain at the N-terminus of Swc5 preferentially binds to the H2A–H2B dimer to facilitate the ejection step of the histone exchange process.

ternatively, the H2A–H2B eviction defect may be compensated for inside the cell by other histone chaperone(s), such as FACT, but probably not Nap1 (Figure 3F) (62). An unstructured acidic region similar to the yeast Swc5-A domain is found in virtually all Swc5 homologs with the exception of plant Swc5 (Supplementary Figure S7A). Perhaps, in plants, the individual histone chaperone proteins play a more dominant role in cooperating with SWR to facilitate the H2A eviction step.

The BCNT core is essential for the histone exchange activity of SWR

Swc5 is well conserved among eukaryotes and is known as BCNT in ruminants, CFDP1 in humans, CP27 in mice, and YETI in flies (58,63,64). BCNT was first identified in ruminants where part of the *Bcnt* gene was duplicated and fused in-frame with an endonuclease domain derived from a bovine-specific retrotransposon, hence the name Bucentaur (65). However, the BCNT-endonuclease fusion is unique to ruminants. The full-length Swc5 homologs found in all eukaryotes, including ruminants, contain the conserved 73-amino-acid BCNT domain (Pfam: PF07572) at the C-terminus (66). The conservation found in the yeast Swc5 is more restricted to a 55-amino-acid core region (57-amino-acid in humans) that is termed the BCNT core domain in Supplementary Figure S7B. Secondary structure informatics indicates strong alpha helical characteristics in the BCNT core, within which a consensus motif [**K**Ψ(T/S)(T/V)**LEK**(**S**/**T**)-xx-**DW**-xx-(**F**/**Y**)] revealed a striking organization of eight highly conserved residues (highlighted in bold) along one face of the predicted alpha helix (Supplementary Figure S11, underlined in pink). Alanine substitutions within the motif in yeast Swc5 (i.e. TT**LEKS**→6A and L**DW**→3A) completely abolished its function *in vivo* and *in vitro.* Similarly, truncating the BCNT core at the C-terminal half also abrogated Swc5 function. These experiments therefore confirm the requirement of the BCNT core in the SWR-mediated remodeling reaction. It is important to point out, however, that the BCNT core is not required for binding the H2A–H2B dimer during the ejection step. Therefore, the Swc5-A domain and the BCNT core domain on the opposite ends of the Swc5 polypeptide play independent roles in the H2A.Z deposition process (Figure 7).

Given the conservation of Swc5 and the central role it plays in the histone exchange reaction of SWR, it was therefore surprising that CFDP1 was absent in the original purification of SRCAP and EP400, the human SWR complexes (67,68). A more recent high-throughput proteomic study has found that CFDP1 co-elutes with SRCAP and DMAP1, which are the human homologs of Swr1 and Swc6, suggesting direct physical interaction (69). However, the molecular role of CFDP1 in H2A.Z deposition remains to be confirmed. Recent studies in flies suggested that YETI plays a chromatin remodeling role (64). However, *Yeti* mutants exhibited a massive chromosomal defect that is associated with loss of all histones (not just H2A.Z) (64). Therefore, the direct role of YETI in H2A.Z deposition remains to be seen.

An updated model of SWR-mediated histone exchange

In yeast cells, the SWR complex is targeted to the proximity of its sites of action, e.g. the promoters, by the affinity of the histone code reader modules to acetylated histone tails (35,36). SWR then engages the +1 nucleosome in a process driven by the affinity of the basic region in Swc2 to the exposed DNA region at the NFR (32). On one hand, the Swc2-Z and the Swr1-Z domains accept the delivery of H2A.Z–H2B by the histone chaperones (Figure 7) (42,60). On the other hand, the ATPase motor on Swr1 engages the DNA on the H2A-containing +1 nucleosome (30). As both histone substrates are bound, the unique structural features of H2A.Z in the dimer and those of H2A in the nucleosome trigger the activation of the Swr1 ATPase, a process requiring Swc5. The DNA translocation activity exerted by the Swr1 ATPase on the tracking DNA strand near the SHL2 position of the nucleosome disrupts the histone-DNA interaction for one of the two H2A–H2B dimers (30). As the H2A–H2B dimer dissociates from what will become a hexasome, the unstructured Swc5-A domain of Swc5 wraps around the dimer to assist the eviction process. Without releasing the hexasome, the H2A.Z–H2B that is held in proximity by the Swc2-Z and/or Swr1-Z is inserted into the apo site on the hexasome in a coupled manner as H2A–H2B is removed (31). The DNA disengages with the ATPase motor and snaps back onto the H2A.Z–H2B dimer, thereby restoring the nucleosomal structure without repositioning the histone octamer. The enzyme dissociates from the resulting heterotypic AZ nucleosome and re-engages with the opposite side of the nucleosome to repeat the histone exchange process (31).

The next challenges will be to continue to tease out the mechanistic steps of the SWR-mediated histone exchange reaction. With regard to Swc5, where is its location in the context of the SWR complex structure, and what structural elements on the H2A–H2B dimer does Swc5 recognize? What role does covalent modifications on Swc5 play, if any, in the histone exchange process? Given the strong conservation of the BCNT domain, is it recognized by other proteins? These are some of the questions that will be addressed in our future studies.

SUPPLEMENTARY DATA

Supplementary Data are available at NAR Online.

ACKNOWLEDGEMENTS

We thank Nancy Hollingsworth for critical reading of the manuscript, Carl Wu for sharing of reagents, Ben Martin for providing the Taq polymerase, Christy Au for assistance in the cloning of the *SWC5* yeast expression vector, our anonymous reviewers for constructive comments, and members of the Luk lab for helpful discussions.

FUNDING

National Institutes of Health [RO1 GM104111 to E.L.]. Funding for open access charge: National Institutes of Health [RO1 GM104111 to E.L.].
Conflict of interest statement. None declared.

REFERENCES

1. Kornberg,R.D. and Lorch,Y. (1999) Twenty-five years of the nucleosome, fundamental particle of the eukaryote chromosome. *Cell*, **98**, 285–294.
2. Arents,G., Burlingame,R.W., Wang,B.C., Love,W.E. and Moudrianakis,E.N. (1991) The nucleosomal core histone octamer at 3.1 A resolution: a tripartite protein assembly and a left-handed superhelix. *Proc. Natl. Acad. Sci. U. S. A.*, **88**, 10148–10152.
3. Luger,K., Mäder,A.W., Richmond,R.K., Sargent,D.F. and Richmond,T.J. (1997) Crystal structure of the nucleosome core particle at 2.8 A resolution. *Nature*, **389**, 251–260.
4. Jiang,C. and Pugh,B.F. (2009) Nucleosome positioning and gene regulation: advances through genomics. *Nat. Rev. Genet.*, **10**, 161–172.
5. Han,M. and Grunstein,M. (1988) Nucleosome loss activates yeast downstream promoters in vivo. *Cell*, **55**, 1137–1145.
6. Kaplan,C.D., Laprade,L. and Winston,F. (2003) Transcription elongation factors repress transcription initiation from cryptic sites. *Science*, **301**, 1096–1099.
7. Rhee,H.S. and Pugh,B.F. (2012) Genome-wide structure and organization of eukaryotic pre-initiation complexes. *Nature*, **483**, 295–301.
8. Krietenstein,N., Wal,M., Watanabe,S., Park,B., Peterson,C.L., Pugh,B.F. and Korber,P. (2016) Genomic Nucleosome Organization Reconstituted with Pure Proteins. *Cell*, **167**, 709–721.
9. Zhou,C.Y., Johnson,S.L., Gamarra,N.I. and Narlikar,G.J. (2016) Mechanisms of ATP-Dependent Chromatin Remodeling Motors. *Annu. Rev. Biophys.*, **45**, 153–181.
10. Bryant,G.O., Prabhu,V., Floer,M., Wang,X., Spagna,D., Schreiber,D. and Ptashne,M. (2008) Activator control of nucleosome occupancy in activation and repression of transcription. *PLoS Biol.*, **6**, 2928–2939.
11. Hartley,P.D. and Madhani,H.D. (2009) Mechanisms that specify promoter nucleosome location and identity. *Cell*, **137**, 445–458.
12. Lorch,Y., Griesenbeck,J., Boeger,H., Maier-Davis,B. and Kornberg,R.D. (2011) Selective removal of promoter nucleosomes by the RSC chromatin-remodeling complex. *Nat. Struct. Mol. Biol.*, **18**, 881–885.
13. Whitehouse,I., Rando,O.J., Delrow,J. and Tsukiyama,T. (2007) Chromatin remodelling at promoters suppresses antisense transcription. *Nature*, **450**, 1031–1035.
14. Yen,K., Vinayachandran,V., Batta,K., Koerber,R.T. and Pugh,B.F. (2012) Genome-wide nucleosome specificity and directionality of chromatin remodelers. *Cell*, **149**, 1461–1473.
15. Albert,I., Mavrich,T.N., Tomsho,L.P., Qi,J., Zanton,S.J., Schuster,S.C. and Pugh,B.F. (2007) Translational and rotational settings of H2A.Z nucleosomes across the Saccharomyces cerevisiae genome. *Nature*, **446**, 572–576.
16. Raisner,R.M., Hartley,P.D., Meneghini,M.D., Bao,M.Z., Liu,C.L., Schreiber,S.L., Rando,O.J. and Madhani,H.D. (2005) Histone variant H2A.Z marks the 5′ ends of both active and inactive genes in euchromatin. *Cell*, **123**, 233–248.
17. Clarkson,M.J., Wells,J.R., Gibson,F., Saint,R. and Tremethick,D.J. (1999) Regions of variant histone His2AvD required for Drosophila development. *Nature*, **399**, 694–697.
18. Faast,R., Thonglairoam,V., Schulz,T.C., Beall,J., Wells,J.R., Taylor,H., Matthaei,K., Rathjen,P.D., Tremethick,D.J. and Lyons,I. (2001) Histone variant H2A.Z is required for early mammalian development. *Curr. Biol. CB*, **11**, 1183–1187.
19. Kobor,M.S., Venkatasubrahmanyam,S., Meneghini,M.D., Gin,J.W., Jennings,J.L., Link,A.J., Madhani,H.D. and Rine,J. (2004) A protein complex containing the conserved Swi2/Snf2-related ATPase Swr1p deposits histone variant H2A.Z into euchromatin. *PLoS Biol.*, **2**, E131.
20. Dhillon,N., Oki,M., Szyjka,S.J., Aparicio,O.M. and Kamakaka,R.T. (2006) H2A.Z functions to regulate progression through the cell cycle. *Mol. Cell. Biol.*, **26**, 489–501.
21. Mizuguchi,G., Shen,X., Landry,J., Wu,W.-H., Sen,S. and Wu,C. (2004) ATP-driven exchange of histone H2AZ variant catalyzed by SWR1 chromatin remodeling complex. *Science*, **303**, 343–348.
22. Santisteban,M.S., Kalashnikova,T. and Smith,M.M. (2000) Histone H2A.Z regulats transcription and is partially redundant with nucleosome remodeling complexes. *Cell*, **103**, 411–422.
23. Zhang,H., Roberts,D.N. and Cairns,B.R. (2005) Genome-wide dynamics of Htz1, a histone H2A variant that poises repressed/basal promoters for activation through histone loss. *Cell*, **123**, 219–231.
24. Dion,M.F., Kaplan,T., Kim,M., Buratowski,S., Friedman,N. and Rando,O.J. (2007) Dynamics of replication-independent histone turnover in budding yeast. *Science*, **315**, 1405–1408.
25. Tramantano,M., Sun,L., Au,C., Labuz,D., Liu,Z., Chou,M., Shen,C. and Luk,E. (2016) Constitutive turnover of histone H2A.Z at yeast promoters requires the preinitiation complex. *eLife*, **5**, e14243.
26. Jeronimo,C., Watanabe,S., Kaplan,C.D., Peterson,C.L. and Robert,F. (2015) The Histone Chaperones FACT and Spt6 Restrict H2A.Z from Intragenic Locations. *Mol. Cell*, **58**, 1113–1123.
27. Wang,F., Ranjan,A., Wei,D. and Wu,C. (2016) Comment on 'A histone acetylation switch regulates H2A.Z deposition by the SWR-C remodeling enzyme'. *Science*, **353**, 358–358.
28. Krogan,N.J., Keogh,M.-C., Datta,N., Sawa,C., Ryan,O.W., Ding,H., Haw,R.A., Pootoolal,J., Tong,A., Canadien,V. *et al.* (2003) A Snf2 family ATPase complex required for recruitment of the histone H2A variant Htz1. *Mol. Cell*, **12**, 1565–1576.
29. Luk,E., Vu,N.-D., Patteson,K., Mizuguchi,G., Wu,W.-H., Ranjan,A., Backus,J., Sen,S., Lewis,M., Bai,Y. *et al.* (2007) Chz1, a nuclear chaperone for histone H2AZ. *Mol. Cell*, **25**, 357–368.
30. Ranjan,A., Wang,F., Mizuguchi,G., Wei,D., Huang,Y. and Wu,C. (2015) H2A histone-fold and DNA elements in nucleosome activate SWR1-mediated H2A.Z replacement in budding yeast. *eLife*, **4**, e06845.
31. Luk,E., Ranjan,A., Fitzgerald,P.C., Mizuguchi,G., Huang,Y., Wei,D. and Wu,C. (2010) Stepwise histone replacement by SWR1 requires dual activation with histone H2A.Z and canonical nucleosome. *Cell*, **143**, 725–736.
32. Ranjan,A., Mizuguchi,G., FitzGerald,P.C., Wei,D., Wang,F., Huang,Y., Luk,E., Woodcock,C.L. and Wu,C. (2013) Nucleosome-free region dominates histone acetylation in targeting SWR1 to promoters for H2A.Z replacement. *Cell*, **154**, 1232–1245.
33. Nguyen,V.Q., Ranjan,A., Stengel,F., Wei,D., Aebersold,R., Wu,C. and Leschziner,A.E. (2013) Molecular architecture of the ATP-dependent chromatin-remodeling complex SWR1. *Cell*, **154**, 1220–1231.

34. Wu,W.-H., Alami,S., Luk,E., Wu,C.-H., Sen,S., Mizuguchi,G., Wei,D. and Wu,C. (2005) Swc2 is a widely conserved H2AZ-binding module essential for ATP-dependent histone exchange. *Nat. Struct. Mol. Biol.*, **12**, 1064–1071.
35. García-Oliver,E., Ramus,C., Perot,J., Arlotto,M., Champleboux,M., Mietton,F., Battail,C., Boland,A., Deleuze,J.-F., Ferro,M. *et al.* (2017) Bdf1 Bromodomains are Essential for Meiosis and the Expression of Meiotic-Specific Genes. *PLOS Genet*., **13**, e1006541.
36. Li,Y., Wen,H., Xi,Y., Tanaka,K., Wang,H., Peng,D., Ren,Y., Jin,Q., Dent,S.Y.R., Li,W. *et al.* (2014) AF9 YEATS domain links histone acetylation to DOT1L-mediated H3K79 methylation. *Cell*, **159**, 558–571.
37. Li,Y., Sabari,B.R., Panchenko,T., Wen,H., Zhao,D., Guan,H., Wan,L., Huang,H., Tang,Z., Zhao,Y. *et al.* (2016) Molecular Coupling of Histone Crotonylation and Active Transcription by AF9 YEATS Domain. *Mol. Cell*, **62**, 181–193.
38. Downs,J.A., Allard,S., Jobin-Robitaille,O., Javaheri,A., Auger,A., Bouchard,N., Kron,S.J., Jackson,S.P. and Côté,J. (2004) Binding of chromatin-modifying activities to phosphorylated histone H2A at DNA damage sites. *Mol. Cell*, **16**, 979–990.
39. Flaus,A., Martin,D.M.A., Barton,G.J. and Owen-Hughes,T. (2006) Identification of multiple distinct Snf2 subfamilies with conserved structural motifs. *Nucleic Acids Res*., **34**, 2887–2905.
40. Ewens,C.A., Su,M., Zhao,L., Nano,N., Houry,W.A. and Southworth,D.R. (2016) Architecture and Nucleotide-Dependent Conformational Changes of the Rvb1-Rvb2 AAA+ Complex Revealed by Cryoelectron Microscopy. *Structure*, **24**, 657–666.
41. Lakomek,K., Stoehr,G., Tosi,A., Schmailzl,M. and Hopfner,K.-P. (2015) Structural basis for dodecameric assembly states and conformational plasticity of the full-length AAA+ ATPases Rvb1 · Rvb2. *Structure*, **23**, 483–495.
42. Liang,X., Shan,S., Pan,L., Zhao,J., Ranjan,A., Wang,F., Zhang,Z., Huang,Y., Feng,H., Wei,D. *et al.* (2016) Structural basis of H2A.Z recognition by SRCAP chromatin-remodeling subunit YL1. *Nat. Struct. Mol. Biol.*, **23**, 317–323.
43. Wu,W.-H., Wu,C.-H., Ladurner,A., Mizuguchi,G., Wei,D., Xiao,H., Luk,E., Ranjan,A. and Wu,C. (2009) N terminus of Swr1 binds to histone H2AZ and provides a platform for subunit assembly in the chromatin remodeling complex. *J. Biol. Chem.*, **284**, 6200–6207.
44. Lin,C.-L., Chaban,Y., Rees,D.M., McCormack,E.A., Ocloo,L. and Wigley,D.B. (2017) Functional characterization and architecture of recombinant yeast SWR1 histone exchange complex. *Nucleic Acids Res.*, doi:10.1093/nar/gkx414.
45. Sikorski,R.S. and Hieter,P. (1989) A system of shuttle vectors and yeast host strains designed for efficient manipulation of DNA in Saccharomyces cerevisiae. *Genetics*, **122**, 19–27.
46. Lowary,P.T. and Widom,J. (1998) New DNA sequence rules for high affinity binding to histone octamer and sequence-directed nucleosome positioning. *J. Mol. Biol.*, **276**, 19–42.
47. Vary,J.C. Jr, Fazzio,T.G. and Tsukiyama,T. (2004) Assembly of yeast chromatin using ISWI complexes. *Methods Enzymol.*, **375**, 88–102.
48. Schwanbeck,R., Xiao,H. and Wu,C. (2004) Spatial contacts and nucleosome step movements induced by the NURF chromatin remodeling complex. *J. Biol. Chem.*, **279**, 39933–39941.
49. Brune,M., Hunter,J.L., Corrie,J.E. and Webb,M.R. (1994) Direct, real-time measurement of rapid inorganic phosphate release using a novel fluorescent probe and its application to actomyosin subfragment 1 ATPase. *Biochemistry (Mosc.)*, **33**, 8262–8271.
50. Park,Y.-J., Chodaparambil,J.V., Bao,Y., McBryant,S.J. and Luger,K. (2005) Nucleosome assembly protein 1 exchanges histone H2A–H2B dimers and assists nucleosome sliding. *J. Biol. Chem.*, **280**, 1817–1825.
51. Ishida,T. and Kinoshita,K. (2007) PrDOS: prediction of disordered protein regions from amino acid sequence. *Nucleic Acids Res*., **35**, W460–W464.
52. Kelley,L.A., Mezulis,S., Yates,C.M., Wass,M.N. and Sternberg,M.J.E. (2015) The Phyre2 web portal for protein modeling, prediction and analysis. *Nat. Protoc.*, **10**, 845–858.
53. De Koning,L., Corpet,A., Haber,J.E. and Almouzni,G. (2007) Histone chaperones: an escort network regulating histone traffic. *Nat. Struct. Mol. Biol.*, **14**, 997–1007.
54. Szerlong,H., Hinata,K., Viswanathan,R., Erdjument-Bromage,H., Tempst,P. and Cairns,B.R. (2008) The HSA domain binds nuclear actin-related proteins to regulate chromatin-remodeling ATPases. *Nat. Struct. Mol. Biol.*, **15**, 469–476.
55. Clapier,C.R., Kasten,M.M., Parnell,T.J., Viswanathan,R., Szerlong,H., Sirinakis,G., Zhang,Y. and Cairns,B.R. (2016) Regulation of DNA translocation efficiency within the chromatin remodeler RSC/Sth1 potentiates nucleosome sliding and ejection. *Mol. Cell*, **62**, 453–461.
56. Cao,T., Sun,L., Jiang,Y., Huang,S., Wang,J. and Chen,Z. (2016) Crystal structure of a nuclear actin ternary complex. *Proc. Natl. Acad. Sci.*, **113**, 8985–8990.
57. Watanabe,S., Radman-Livaja,M., Rando,O.J. and Peterson,C.L. (2013) A histone acetylation switch regulates H2A.Z deposition by the SWR-C remodeling enzyme. *Science*, **340**, 195–199.
58. Iwashita,S., Suzuki,T., Yasuda,T., Nakashima,K., Sakamoto,T., Kohno,T., Takahashi,I., Kobayashi,T., Ohno-Iwashita,Y., Imajoh-Ohmi,S. *et al.* (2015) Mammalian Bcnt/Cfdp1, a potential epigenetic factor characterized by an acidic stretch in the disordered N-terminal and Ser250 phosphorylation in the conserved C-terminal regions. *Biosci. Rep.*, **35**, e00228.
59. Swaney,D.L., Beltrao,P., Starita,L., Guo,A., Rush,J., Fields,S., Krogan,N.J. and Villén,J. (2013) Global analysis of phosphorylation and ubiquitylation cross-talk in protein degradation. *Nat. Methods*, **10**, 676–682.
60. Hong,J., Feng,H., Wang,F., Ranjan,A., Chen,J., Jiang,J., Ghirlando,R., Xiao,T.S., Wu,C. and Bai,Y. (2014) The catalytic subunit of the SWR1 remodeler is a histone chaperone for the H2A.Z–H2B dimer. *Mol. Cell*, **53**, 498–505.
61. Zhou,Z., Feng,H., Hansen,D.F., Kato,H., Luk,E., Freedberg,D.I., Kay,L.E., Wu,C. and Bai,Y. (2008) NMR structure of chaperone Chz1 complexed with histones H2A.Z–H2B. *Nat. Struct. Mol. Biol.*, **15**, 868–869.
62. Kemble,D.J., McCullough,L.L., Whitby,F.G., Formosa,T. and Hill,C.P. (2015) FACT disrupts nucleosome structure by binding H2A–H2B with conserved peptide motifs. *Mol. Cell*, **60**, 294–306.
63. Diekwisch,T.G., Marches,F., Williams,A. and Luan,X. (1999) Cloning, gene expression, and characterization of CP27, a novel gene in mouse embryogenesis. *Gene*, **235**, 19–30.
64. Messina,G., Damia,E., Fanti,L., Atterrato,M.T., Celauro,E., Mariotti,F.R., Accardo,M.C., Walther,M., Vernì,F., Picchioni,D. *et al.* (2014) Yeti, an essential Drosophila melanogaster gene, encodes a protein required for chromatin organization. *J. Cell Sci.*, **127**, 2577–2588.
65. Nobukuni,T., Kobayashi,M., Omori,A., Ichinose,S., Iwanaga,T., Takahashi,I., Hashimoto,K., Hattori,S., Kaibuchi,K., Miyata,Y. *et al.* (1997) An Alu-linked repetitive sequence corresponding to 280 amino acids is expressed in a novel bovine protein, but not in its human homologue. *J. Biol. Chem.*, **272**, 2801–2807.
66. Iwashita,S. and Osada,N. (2011) Bucentaur (Bcnt) gene family: gene duplication and retrotransposon insertion. *In Gene Duplication. InTechOpen*, 383–400.
67. Doyon,Y., Selleck,W., Lane,W.S., Tan,S. and Côté,J. (2004) Structural and functional conservation of the NuA4 histone acetyltransferase complex from yeast to humans. *Mol. Cell. Biol.*, **24**, 1884–1896.
68. Jin,J., Cai,Y., Yao,T., Gottschalk,A.J., Florens,L., Swanson,S.K., Gutiérrez,J.L., Coleman,M.K., Workman,J.L., Mushegian,A. *et al.* (2005) A mammalian chromatin remodeling complex with similarities to the yeast INO80 complex. *J. Biol. Chem.*, **280**, 41207–41212.
69. Havugimana,P.C., Hart,G.T., Nepusz,T., Yang,H., Turinsky,A.L., Li,Z., Wang,P.I., Boutz,D.R., Fong,V., Phanse,S. *et al.* (2012) A census of human soluble protein complexes. *Cell*, **150**, 1068–1081.